Prediction of Square Footing Settlement under Eccentric Loading on Gypseous Soil through Proposed Surface for Dry and Soaked States

Dr. Bushra S. Z. Albusoda
Building and Construction Engineering Department, University of Baghdad/ Baghdad
Email:albusoda@yahoo.com
Dr.Abdul-Kareem E.
Building and Construction Engineering Department, University of Baghdad/ Baghdad
R. S.Hussein
Building and Construction Engineering Department, University of Baghdad/ Baghdad

ABSTRACT

Gypseous soils as any other soils deform under loading, this deformation differs greatly between its dry state and its soaked state. This deformation also differs when the loading is applied with eccentricity.

An experimental work was conducted on a square footing model (100 mm $\times$ 100 mm) above gypseous soil 450 mm thick. Loading was applied at the center of the footing (e/B = 0) and at an eccentricity of (e/B = 0.05, 0.1, 0.15, 0.2) for its dry state and its soaked state. Settlement was obtained at the center and at the base soil of the footing for each state.

The data obtained was normalized and a proposed surface was obtained for each of the two states (dry and soaked) and at two places (center and edge). Four proposed equations were obtained represented four cases of research i) Dry center, ii) Dry edge, iii) Soaked center, and iv) Soaked edge. The four equations showed very good agreement with the data obtained from the experiment.

Artificial Neural Network model was also used to obtain a neural network representing the proposed surface for the abovementioned four cases and also a very good agreement was obtained.

It is concluded that a proposed surface for the central and eccentric loading on square footing for gypseous soil showed a good agreement with the experimental data and therefore may be used for settlement prediction.

Key words: Gypseous Soil, Settlement Prediction, Square Footing, Artificial Neural Network (ANN).

تنبؤ هطول الاساس المربع تحت الحمل اللامركزي على التربة الجبسية خلال السطح المقترح للحالات الجافة والرطبة

الخلاصة

التـرب الجبسية كغيرهـا مـن التـرب ممكـن ان تتعـرض الـى التشـوهات تحـت الاحمـال، هـذه التشـوهات تختلـف بشكل كبيـر بـين الحالـة الجافة للتربـة والحالـة المغمـورة بالميـاه، وكذلك بـاختلاف الاحمال خاصة عند تعرض التربة للاحمال غير المركزية.

تم اجراء تجارب مختبرية على نموذج لاساس مربع بابعاد 100 ملم × 100ملم فوق تربة جبسية سمكها 450 ملم. تم تسليط الحمل في مركز النموذج وكذلك بشكل لامركزي وبنسب مختلفة لكلا الحـالتين الجافة والمغمـورة وتم الحصـول على القراءات المطلوبـة في مركز النموذج وعلى طرف النموذج.

تم تعديـل القراءات للحصـول على سطح خـاص لكـل حالـة (جافة ومغمـورة) وكذلك لكل من (المركز والطرف). وعليه فقد تم الحصـول علـى اربعـة اسطح مقترحـة أ) جـاف مركز ب) جـاف طرف جـ) مغمور مركز د) مغمور طرف. منهـا تم الحصـول علـى اربعـة معـادلات مقترحـة لهـذه الاسطح التـي اعطت توافق جيد جدا مع البيانات التي تم الحصول عليها من التجارب العملية.

كذلك تـم استخدام الشبكات العصبية كطريقة اخرى للحصـول على اسطح مقترحـة للحـالات الاربعـة المذكورة وكذلك بينت النتائج التوافق العالي مع البيانات التي تم الحصول عليها من التجارب.

من هذا يمكن القول بـان اقتـراح اسطح لتخمين الهبوط فـي التـرب الجبسية لكل من الحـالات الجافة والمغمورة وفي مركز الاساس وعلى الطرف اعطى نتائج متوافقة بشكل جيد جدا مع البيانـات التي تم الحصول عليها من التجارب.

INTRODUCTION

G ypsies soil is that soil which contains enough gypsum (CaSO $_4$ .2H $_2$ O) that affect on the behavior of soil. Gypsum has specific gravity of (2.32) and its solubility of gypsum in water is (2gm/liter) at 20 °C, but the amount of dissolved gypsum can be much greater if water contains some salts (Hesse, 1971 and Khan, 2005).

In Iraq, gypsies soils are mostly found in Mosul, Baiji, Tikrit, Sammera, North West of Baghdad, Anna, Heet, Ramadi, Falloja and they may be presented in other regions (Al-Jananbi, 2002). Gypseous soils are classified as collapsing soils. This is due to the fact that gypsum provides an apparent cementation when the soil is dry but the intrusion of the water causes dissolution and softening leading generally to a serious structural collapse (Razouki, et al, 1994).

Many problems have been noticed in different structures constructed on gypseous soils in Iraq. For examples, the damage cases and collapse occurred in the soil under the foundations of the houses in AL-Thawrra Hai, 1969, in Mosul City (Al-Busoda, 1999). Other problems of gypseous soil are cavities created under the foundation of Mosul Dam due to the continuous dissolution of gypsum under the dam (Nashat, 1990).One of the problems resulting due to the dissolve of gypsum is the damages that occurred in Al-Anbar University in Al-Ramdi City, see Figure (1), and cracks were pointed in Dijla Hospital, in Tikriin Figure (2).

Eng. & Tech. Journa , Vol.31.Part(A) , No.20,2013 Prediction of Square Footing Settlement under
Eccentric Loading on Gypseous Soil through
Proposed Surface for Dry and Soaked States

MATERIALS AND EXPERMENTIAL WORK

A series of tests was performed on the gypseous soil according to ASTM procedures. In this study, gypseous soil can be classified as (SC) according to the Unified Soil Classification System. The grain size distribution curves of gypseous soil is shown in Figure (3). The minimum unit weight of gypseous soil tested was determined according to the test described by (Head, 1984), it is widely accepted as standard test for sandy soils and the maximum unit weight of gypseous soil tested was determined according to ASTM D-64T (Bowles, 1988). Field unit weight of gypseous soil was determined by a field test (Sand Cone Method). This test was performed according to (ASTM D1556-00). The results of the maximum and minimum unit weights of gypseous soils are (14.10) kN/m^3 and (10.75) kN/m^3 respectively. Tables (1 and 2) show the physical and chemical properties of the selected gypseous soil.

Qualitative identification of both, clay and non clay minerals, in a soil can be made using X-ray diffraction which is the most widely used method for identification of fine grained soil minerals and the study of their crystal structure. This test was conducted by the State Company for Geological Survey and Mining (Ministry of Industry and Minerals). Table (3) shows the results of X-ray diffraction analysis of gypseous soil.

Tests were carried out in a steel box with inside dimensions of (600) mm width (600) mm length and (500) mm height. The sides and bottom were made of (5) mm thickness plate. One face of the box was made from plexiglass with dimensions (300) mm width and (300) mm length. The test box was placed over (800) mm width and (1000) mm length of strong steel base, which was connected to a stiff loading frame.The frame consists of two columns of steel channels, which in turn bolted to a loading platform. This platform was allowed to slide along the columns and can be fixed at any desired height by means of slotting spindles and holes provided at different intervals along the columns.

The model footing was made from steel plate of thickness (3) mm and having dimensions $(100*100)$ mm^2. The footing was connected to suitable steel wings to facilitate the measurement of settlement. A hydraulic jack of (10) tons capacity was used to apply the axial system loading on footing. The load on the footing was measured using proving ring of (20) kN capacity, while the settlement was measured by two dial gauges (0.01) mm fixed on the middle of the footing by two magnetic holders. The water level in the test box was kept constant during the test. In order to obtain a uniform density of soils, hopper was used with height (75) mm and having valve to control the sand raining by hand. Figure (4) shows the general view of testing equipment.

TEST PROCEDURE FOR MODEL LOADING TEST
Placement of Soil

The density of the gypsies soils used through the experiments was controlled by means of the raining technique. This technique includes raining the soil by different heights of drop that give different placing densities. Many investigators such as Lee, et al (1973), Denver, (1983), and Sanjeev, (2007) used this technique. The relations between heights of drop, placement density, void ratio and relative density of

gypseous soils is shown in Figure (5). It was decided to employ unit weight (12.9) kN/m^3 of gypseous soils, which corresponds to the height of drop of (29) cm.

Bearing Capacity Test Procedure

The test was conducted by using non repetitive static plate load test method according to the procedure of ASTM D1194-94. The bearing capacity was determined for various thicknesses of gypseous soil beds. In each test, the gypseous soil was placed in layers (5) cm thick. The placement density was controlled using raining technique. The gypseous soil was carefully spreaded in two perpendicular directions to ensure a uniform density. When the final layer was placed, the surface was carefully leveled straight edge. Then, the foundation was fixed in the center of the test box in x and y directions in eccentric loading and then the two magnetic holders using dial gauges in the edge of the box was connected. The load was continuously applied through the hydraulic jack. The applied load was obtained from the proving ring reading while the settlement was measured by the dial gauges.

When soaking is conducted, the steel box is left for (24) hours to ensure that all the soil was completely soaked. The application of load was continued up to failure. The failure was indicated by the increase of settlement at a constant magnitude of load intensity.

Figures (6 and 7) illustrate the load–settlement at center and edge curves for dry gypseous soil under different eccentricity values (e = 0.05B, 0.1B, 0.15B, 0.2B), respectively. These results show that the behavior of load–settlement curves seem to be like the general shear failure curve.

This behavior was expected because the soil was in dense state. The main problem of gypseous soil appeared during soaking because of the dissolution of gypsum. Therefore, many tests are conducted on gypseous soil during soaking under different values of eccentricity.

From Figures (8and 9), it can be observed that there is a high decrease in bearing capacity after soaking compared with dry state.The maximum load carrying increased with the decrease of eccentricity (e = 0.05 B), and decreased when (e = 0.2 B).

For small value of eccentricity, the difference in settlement between edge and center dial guage is also small. But this difference increased with the increase in eccentricity.

The data obtained from experimental work were normalized where

　　a- Normalized loading was obtained by obtaining $q/_{qult}$ where
　　　　q = load, and
　　　　q_{ult} = ultimate loading as shown in Table (4).
　　b- Normalized settlement by obtaining s/D where
　　　　s= settlement in mm,
　　　　D= Soil depth = 450 mm
　　c- Normalized eccentricity by obtaining e/B where
　　　　e = eccentricity
　　　　B= footing breadth.

The observed values may be considered high with respect to predicated values obtained from theoretical (Terzaghi equation). Same observation was found by Al-Jebouri, (1986). Several suggestions were made to use ($\emptyset \cong \emptyset p \cong 1.1\emptyset t$) Das, (2008). The value of ($\emptyset$) determined by triaxial test and multiplied by (1.1) was used in the calculation of theoretical equation.

Eng. & Tech. Journa , Vol.31.Part(A) , No.20,2013   **Prediction of Square Footing Settlement under
Eccentric Loading on Gypseous Soil through
Proposed Surface for Dry and Soaked States**

Figures (10 and 11) represent normalized curves for the dry state of soil at center and edge of the footing respectively, and Figures (12 and 13) represent normalized curves for the Soaked state of soil at center and edge of the footing respectively.

Figures (14 and 15) represent the surfaces obtained from the normalized data for the dry state for s/D at center and at the edge respectively, where the third dimension used was the e/B axis. Figures (16 and 17) are for the soaked state at center and edge respectively.

Surface fitting using surface equation

To obtain a best fit surface equation, a computer program (LABFIT) was used and the best equation for each case was found. The symbols used were:

$y = s/D$, $x_1 = q/qult$, $x_2 = e/B$

Case 1: Dry state at center

Equation 1 was obtained and the best fit surface is shown in Figure (18)

$$y = \frac{a + bx_2}{1 + cx_1 + dx_1^2} \qquad \text{... (1)}$$

a=0.1430E-02, b=-0.4557E-02, c=-0.1721E+01, d=0.7839E+00, $R^2 = 0.973$

Case 2: Dry state at edge

Equation 2 was obtained and the best fit surface is shown in Figure (19).

$$y = \frac{a + x_2}{b + cx_1} + d \qquad \text{... (2)}$$

a=0.1515E+01, b=0.1254E+03, c=-0.8277E+02, d=-0.1327E-01, $R^2 = 0.9817$

Case 3: Soaked state at center

Equation 3 was obtained and the best fit surface is shown in Figure (20).

$$y = \frac{a + b * x_2}{1 + cx_1 + dx_1^2} \qquad \text{...(3)}$$

a=0.1761E-02, b=-0.8856E-02, c=-0.1662E+01, d=0.7407E+00, $R^2 = 0.929$

Case 4: Soaked state at edge

Equation 4 was obtained and the best fit surface is shown in Figure (21).

$$y = \frac{a + x_1}{b + cx_2} + dx_2 \qquad \text{... (4)}$$

a=-0.7803E-03, b=0.2072E-01, c=-0.4244E+01, d=0.2144E+02, $R^2 = 0.9389$

Artificial Neural Network (ANN)

Artificial neural network method was also used to predict the factor s/D using q/qult and e/B as the input data for prediction, the Levenberg-Marquardt back propagation method of training was used with Hyperbolic tangent sigmoid and pure linear activation function. a neural network of 2 hidden layers each containing 20 neurons was used. The surface obtained were illustrated in Figures 22 to 25.

DISCUSSION

The procedure used to predict the settlement of a square footing model depends mainly on transforming the experimental data into its equivalent normalized surface. Where the dimensionless factors e/B, q/qult, and s/D were used.

Two methods were implemented to find the best surface that can describe the relation among the three factors mentioned.

The first method was to find the best fit surface equation using the computer program LABFIT which can find the most suitable equation that can describe the surface with the maximum value of correlation coefficient as shown in Table (7).

It is noticed that the surface describing the normalized settlement at center tend to have the form

$$y = \frac{a + b * x_2}{1 + cx_1 + dx_1^2} \qquad \qquad \dots(5)$$

Where the surface describing the normalized settlement at edge tend to have the form

$$y = \frac{a + x_1}{b + cx_2} + dx_2 \qquad \qquad \dots(6)$$

The second method was to use Artificial Neural Netwok (ANN). The network was trianed to predict the surface for each of the four cases. The results of the correlation coeffiecints are shown in Table (7).

It is noticed that the ANN procedure gave greater correlation coefficients compared to the surface equation obtained from LABFIT.

CONCLUSIONS AND RECOMMENDATIONS

From the data analysis and reviewing the correletion coefficints and the figures above, it is concluded that:

1. Normalized data (e/B, s/D, q/qult) can be described as surface due to smooth translation of the values of normalized settlement (s/D) that helped in predicting a proposed equation for each of the four cases (dry-center, dry-edge, soaked-center, and soaked-edge) with a ver good correleation coefficients.
2. Using ANN can also describe a proposed surface with very good correleation coefficients.

Though it is recommended that this work if further investigated, to confirm that a general surface for settlement prediction may be obtained.

REFERENCES

[1]. Al-Busoda, B. S. Z., (1999) "Studies on the Behavior of Gypseous Soil and its Treatment During Loading", M.Sc. Thesis, Civil Engineering Department, University of Baghdad.

[2]. Al-Janabi, F. H., (2002) "Assessment of Non-Linear Behavior of Fuel Oil Treated Reinforced Gypseous Soils", M.Sc. Thesis, Building and Construction Engineering Department, University of Technology, Baghdad.

[3]. Annual Book of ASTM Standard, Vol.04.08, (2000).

[4]. Bowles, J. E., (1988) "Foundation Analysis and Design", Fourth Edition, McGraw-hill, New York.

[5]. Das, B. M., (2008) "Advanced Soil Mechanics", Third Edition, Brooks/Cole. New York.

[6]. Denver, H. et al, (1983) "Reinforcement of Cohesionless Soil by PVC-Grid", Improvement of Ground, Proc, of the Eighth European Conference on Soil Mech and Found Eng, Vol.2, PP.481-489.

[7]. Head, K. H., (1984-1986) "Manual of Soil Laboratory Testing" Volume 1,2, and 3. Prentch Press, London.

[8]. Hesse, P.R. (1971) "A Text Book of Soil Chemical Analysis". Chemical analysis Publishing Co., Int., New York.

[9]. Khan, M.A.J., (2005) "Effect of Compaction on The Behavior of Kirkuk Gypseous Soil" M.Sc. Thesis, Civil Engineering Department, University of Baghdad.

[10]. Lee, K. L., Adams, B. D., and Vagneron, J. M. J., (1973) "Reinforced Earth Retaining Walls", Journal Soil Mech. Found. Div., Pro, ASCE, Vol.9, No.Sm10, PP.745-763.

[11]. Nashat, I.,H., (1990) "Engineering Characteristics of Some Gypseous Soils in Iraq", Ph.D. Thesis, Civil Engineering Department, University of Baghdad.

[12]. Razouki, S. S., Al-Omari, R. R., Nashat, I. H., Razouki, H. F. and Khalid, S. (1994) "The Problems of Gypsiferous Soils in Iraq." Symposium on gypsiferous soils and their effect on structures, NCCL, Baghdad.

[13]. Sanjeev, M., (2007) "Effect of Wall Thickness on Plugging of Open Ended Steel Pipe Piles in Sand", ASCE, Vislttttp://www.ascelibrary.org. PP.1-16.

Table (1) Physical Properties of Gypseous Soil.

w_c , (%)	3.2
g_{field} , (kN/m^3)	12.9
G_S	2.41
L.L, (%)	36
P.L, (%)	22
k, (cm/sec), (variable head)	$2.358*10^{-5}$
C_u	2.12
C_C	1.46

Table (2) Chemical Properties of Gypseous Soil.

Chemical Composition	Percentage, (%)
SO_3	20.86
Cl	0.053
Gypsum Content	45
T.S.S	47.4
$CaCO_3$	13.30
Organic Content	0.44
pH	8.8-9.2

Eng. & Tech. Journa , Vol.31.Part(A) , No.20,2013   **Prediction of Square Footing Settlement under**
Eccentric Loading on Gypseous Soil through
Proposed Surface for Dry and Soaked States

Table (3) Mineralogical Composition of Gypseous Soil.

Non-Clay Minerals	Clay Minerals
$CaSO_4.2H_2O$ (Gypsum)	Polygosikte
$CaCO_3$ (Calcite)	
Quartz	
Dolomite	

Table (4) Experimental and Theoretical Ultimate Bearing
Capacity of (Dry and Soaked States).

Ultimate Bearing Capacity, (kPa)	Theoretical	Experimental Results
Dry State	561.84	660
Soaked State	135.07	205

Table (5) Experimental and Theoretical Ultimate Bearing Capacity of (Dry
State) under Different Values of Eccentricities.

Ultimate Bearing Capacity, (kPa)	Theoretical	Experimental Results
Bearing Capacity at (e=0.05 B)	551.23	648
Bearing Capacity at (e=0.1 B)	540.63	635
Bearing Capacity at (e=0.15 B)	530	565
Bearing Capacity at (e=0.2 B)	519.40	540

Table (6) Experimental and Theoretical Ultimate Bearing Capacity
of (Soaked State) under Different Values of Eccentricities.

Ultimate Bearing Capacity, (kPa)	Theoretical	Experimental Results
Bearing Capacity at (e=0.05)	134.85	187.5
Bearing Capacity at (e=0.1 B)	134.60	182
Bearing Capacity at (e=0.15 B)	134.36	140
Bearing Capacity at (e=0.2 B)	134.14	125

Table (7) Correlation coefficints obtained (R).

	Dry (Center)	Dry (Edge)	Soaked (Center)	Soaked (Edge)
Labfit	0.98665	0.990833	0.964212	0.968968
ANN	0.997485	0.998709	0.976517	0.988338

Eng. & Tech. Journa , Vol.31.Part(A) , No.20,2013   **Prediction of Square Footing Settlement under
Eccentric Loading on Gypseous Soil through
Proposed Surface for Dry and Soaked States**

**Figure (1) Collapse of a building in Al-Ramadi
City, (From Tawfeeq, 2009).**

**Figure (2) Cracks of Walls in Dijla Hospital in Tikrit
City,(From Tawfeeq, 2009).**
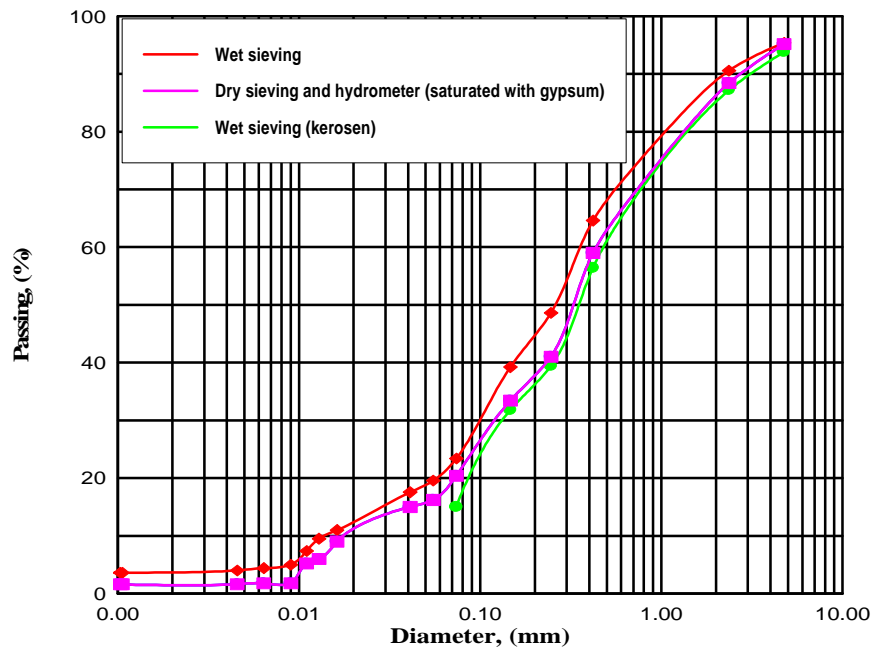
Figure (3) Grain Size Distribution Curves of Gypseous Soil.

Figure (4) General View of Testing Equipment.
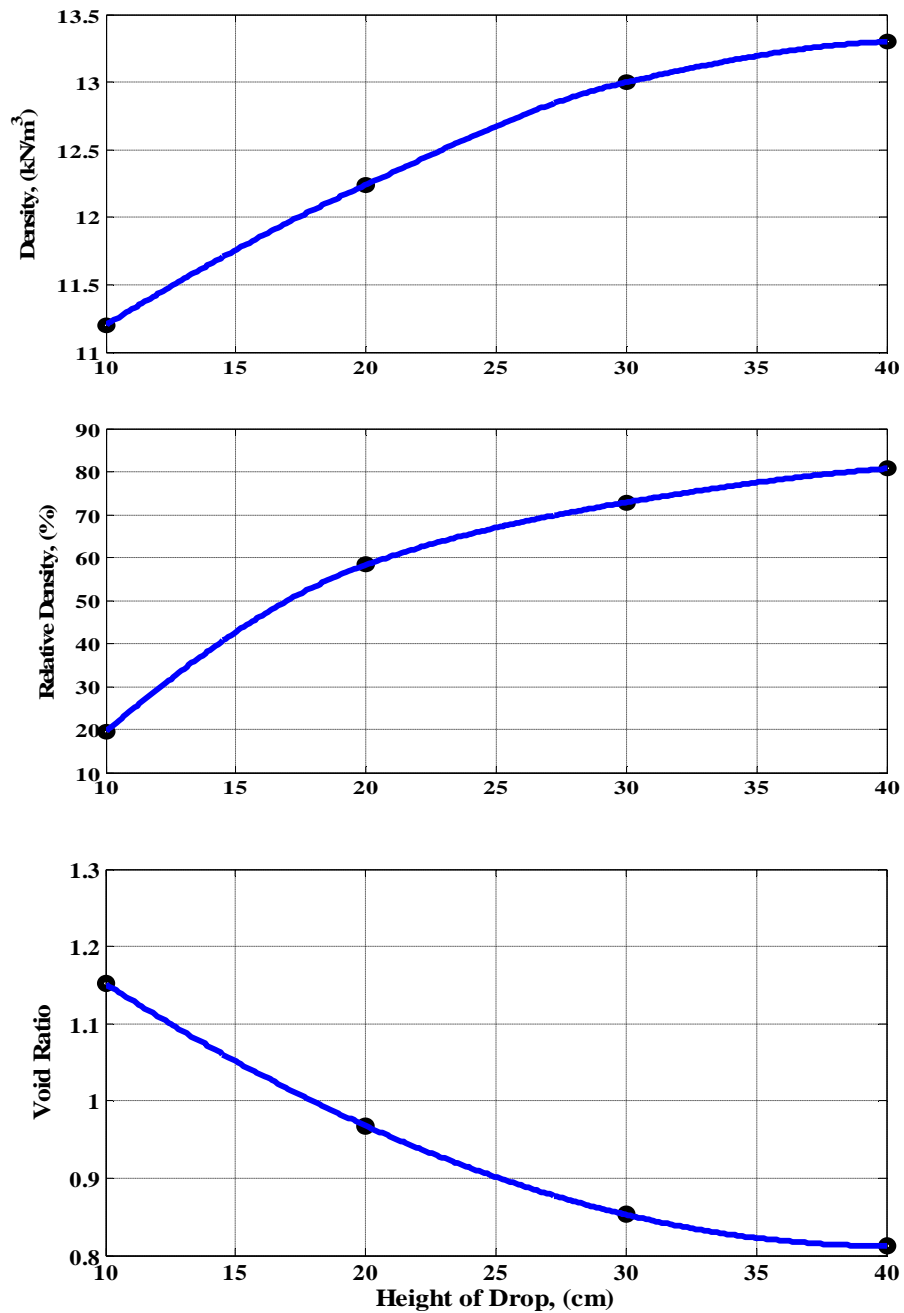
Figure (5) Density Calibration Curves for Gypsies Soil by Raining Technique.
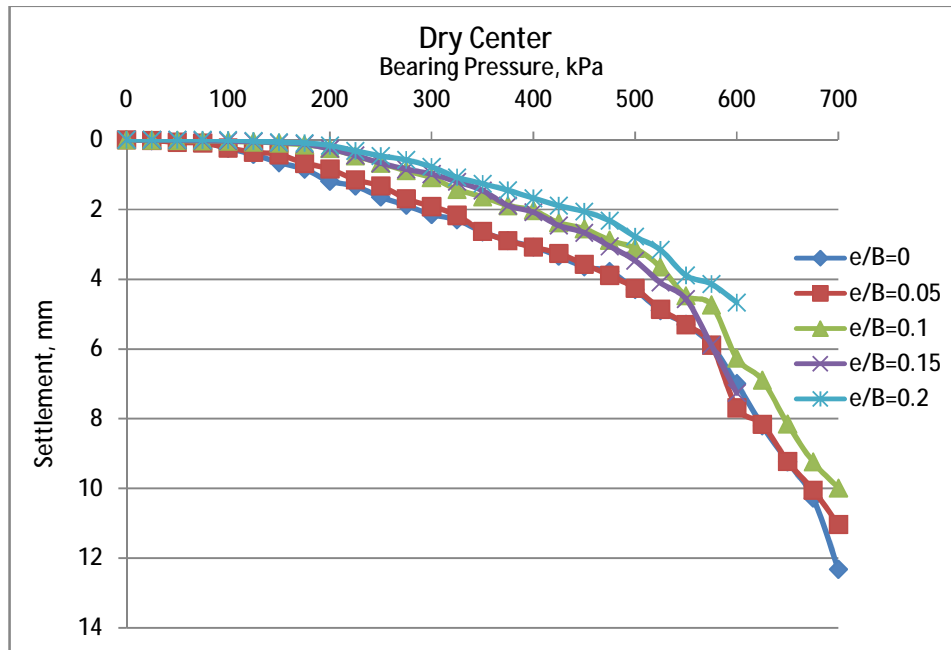
Figure (6) Pressure - Settlement Curves for Gypseous Soil at Dry State (Center).
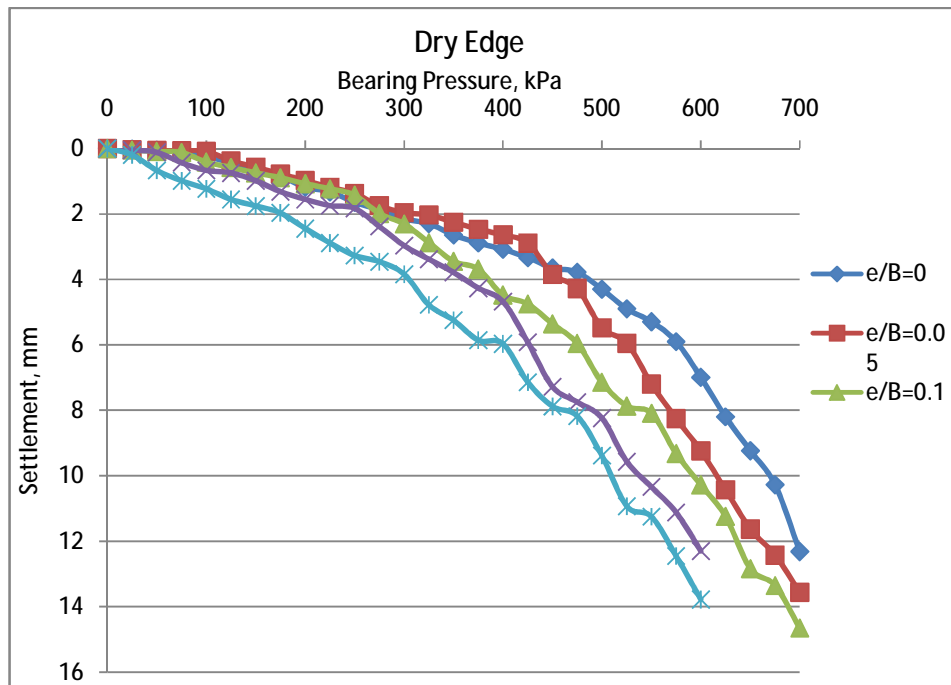
Figure (7) Pressure - Settlement Curves for Gypseous Soil at Dry State (Edge).

*Eng. & Tech. Journa , Vol.31.Part(A) , No.20,2013* Prediction of Square Footing Settlement under
Eccentric Loading on Gypseous Soil through
Proposed Surface for Dry and Soaked States
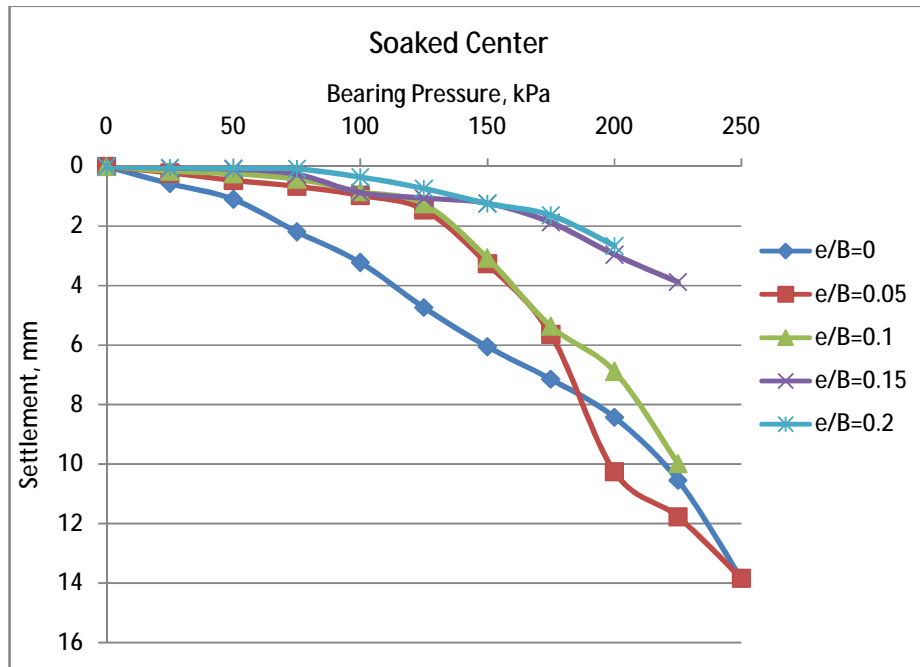
**Figure (8) Pressure - Settlement Curves for Gypseous Soil at
Soaked State (Center).**
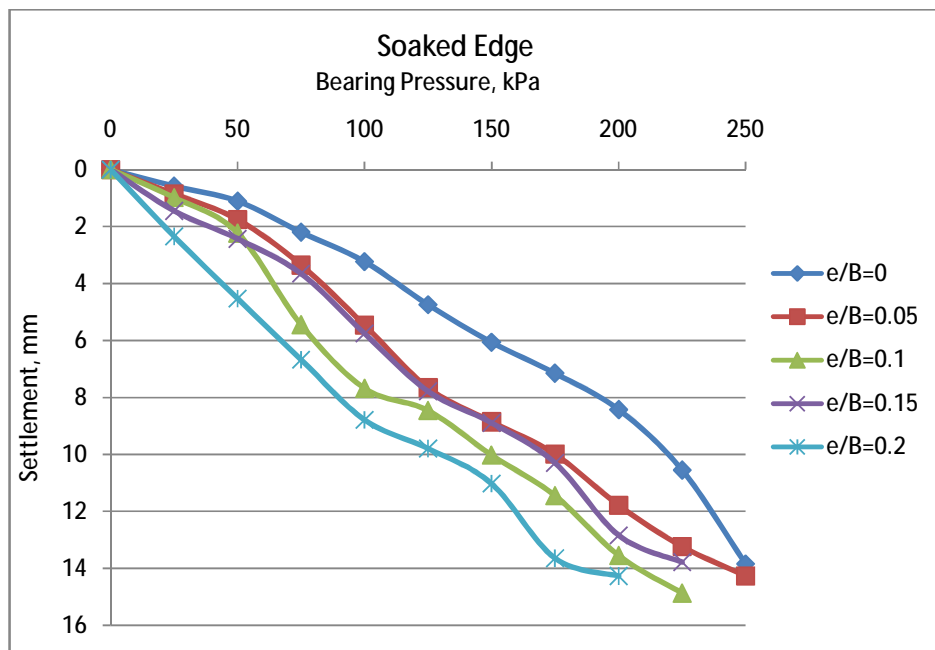
**Figure (9) Pressure - Settlement Curves for Gypseous Soil at
Soaked State (Edge).**
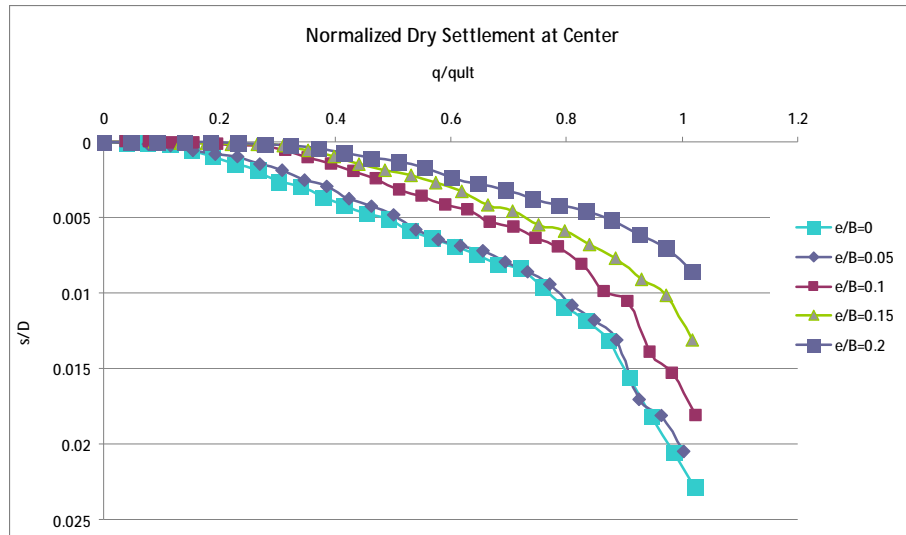
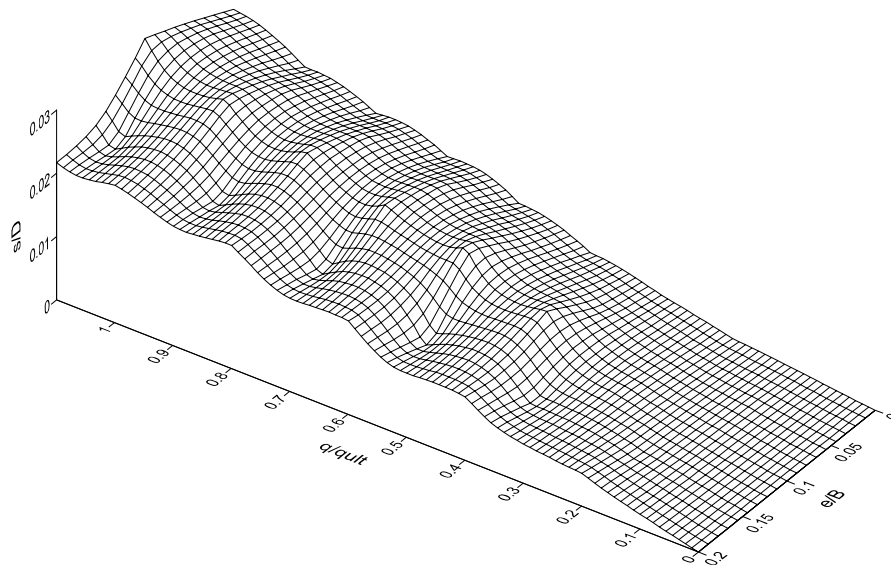**Figure (10) Normalized Pressure –Settlement Curves for Gypseous Soil at Dry State (Center).**
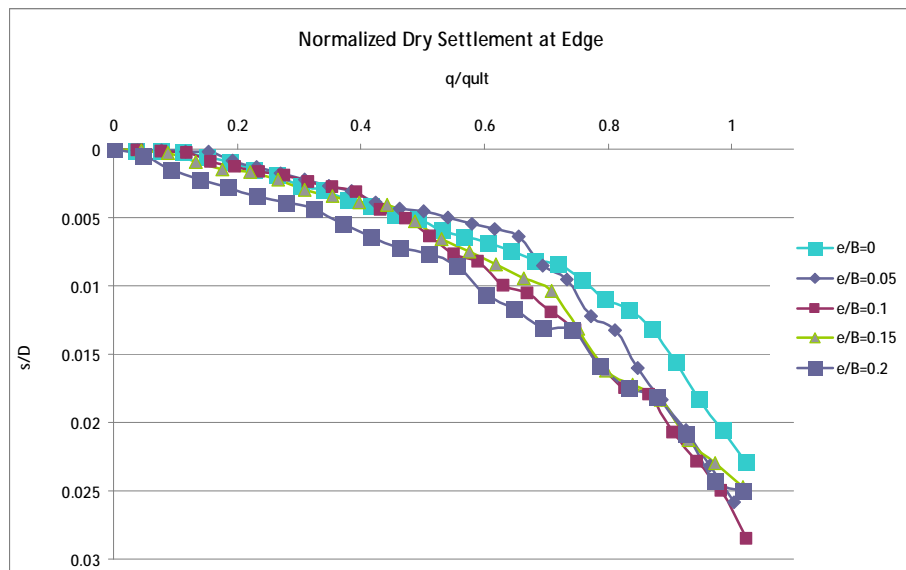
Figure (11) Normalized Pressure –Settlement Curves for Gypseous Soil at Dry State (Edge).
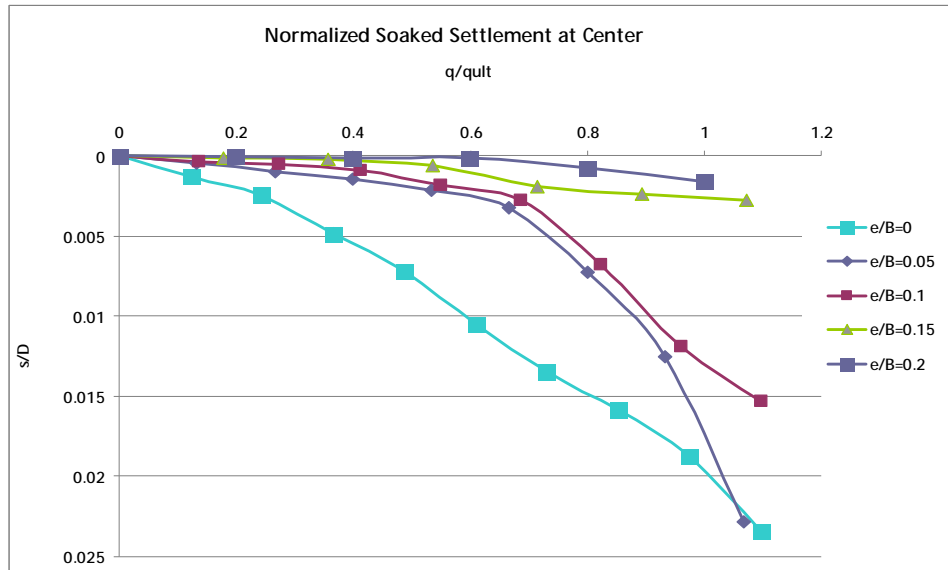
Figure (12) Normalized Pressure –Settlement Curves for Gypseous Soil at Soaked State (Center).
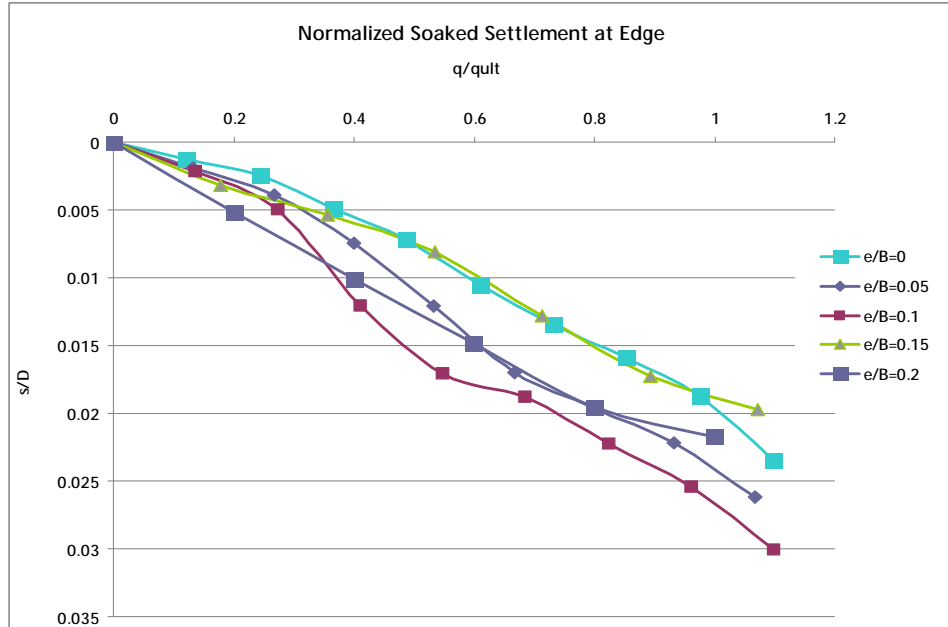
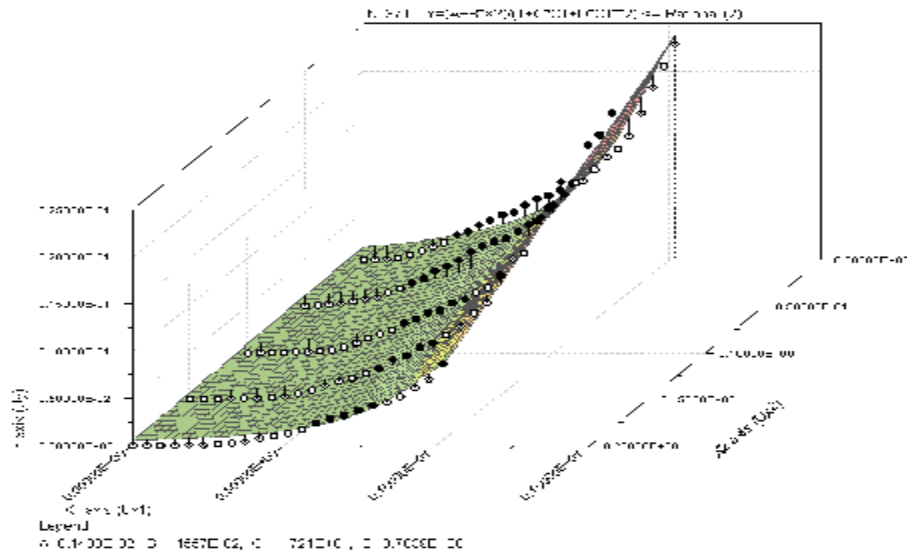**Figure (13) Normalized Pressure –Settlement Curves for Gypseous Soil at Soaked State (Edge).**
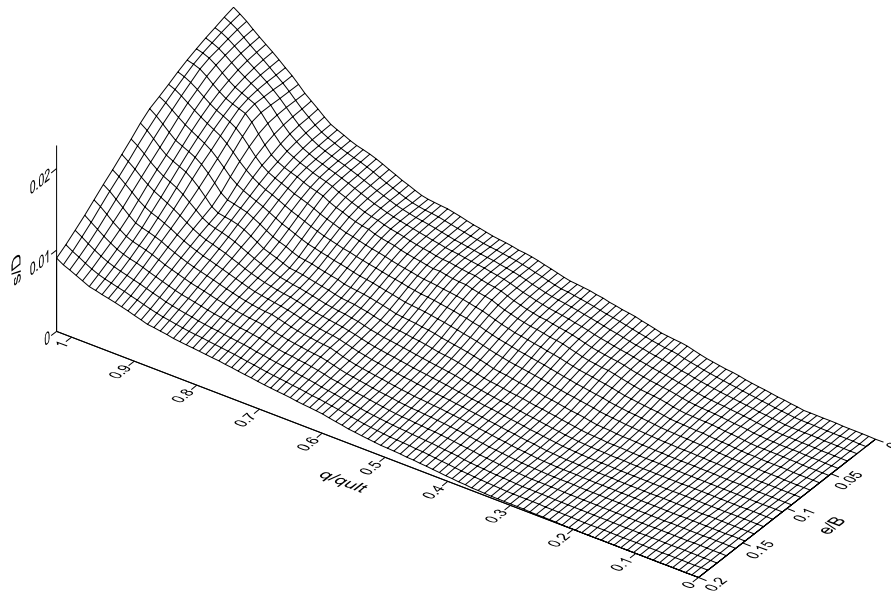
Figure (14) Normalized Pressure –Settlement Surface for Gypseous Soil at Dry State (Center).
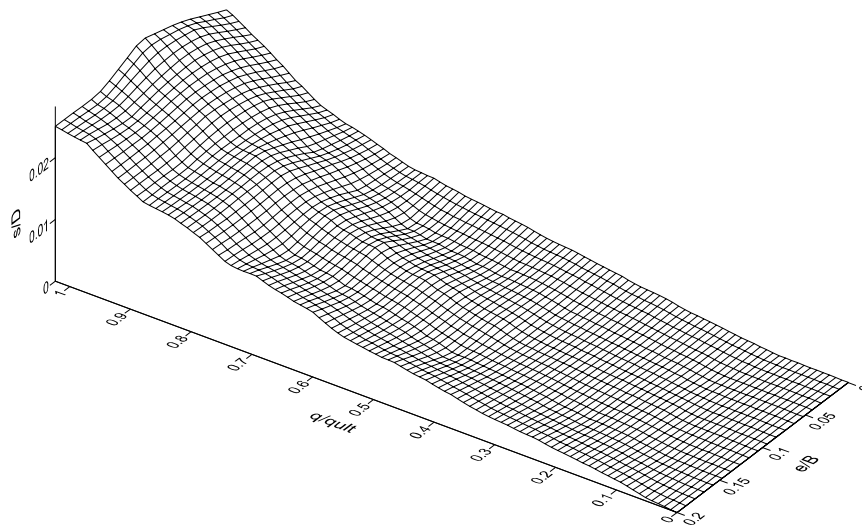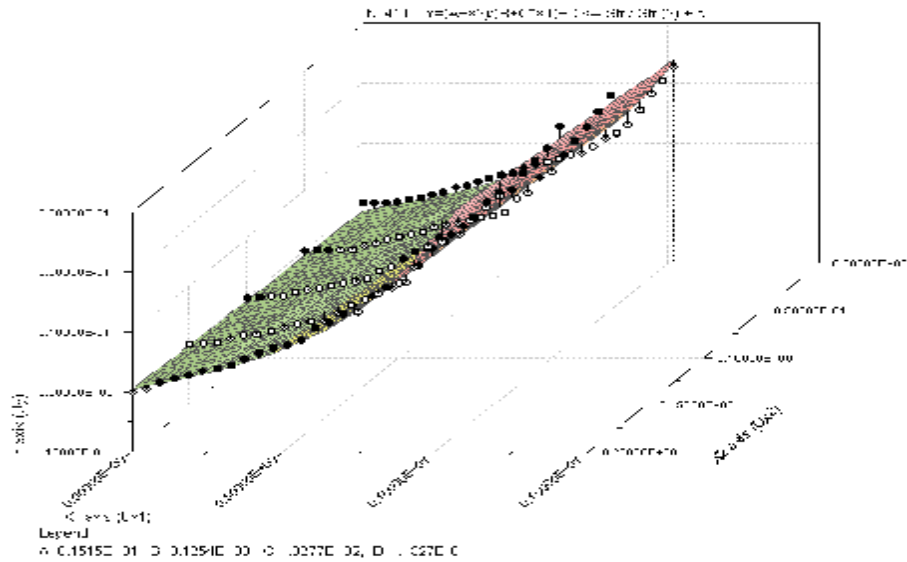
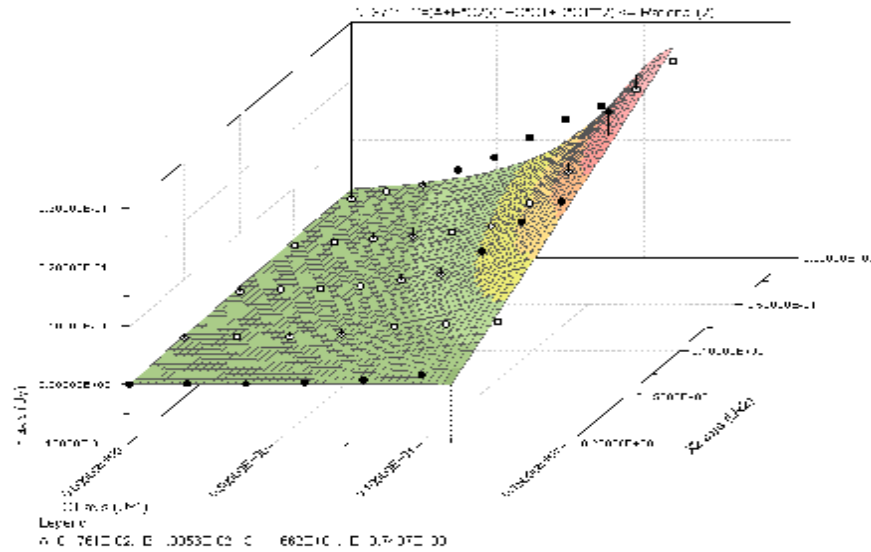**Figure (15) Normalized Pressure –Settlement Surface for Gypseous Soil at Dry State (Edge).**
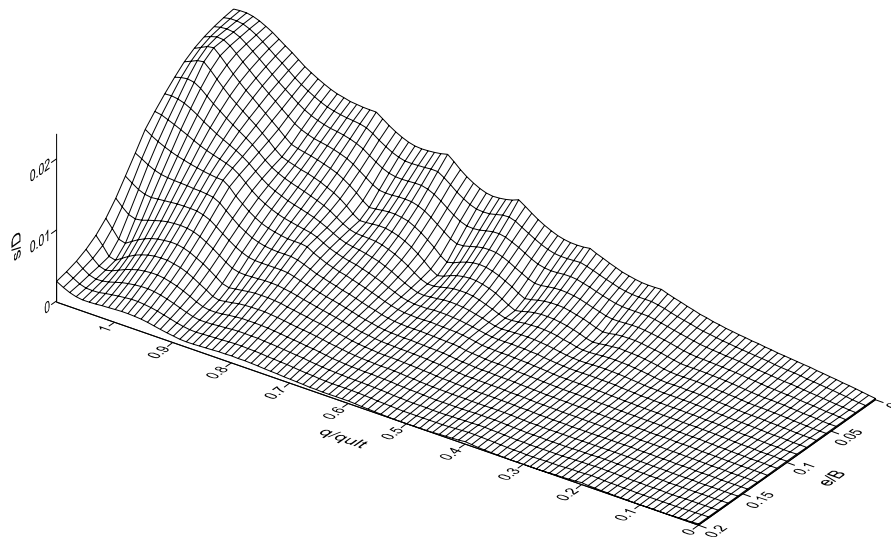
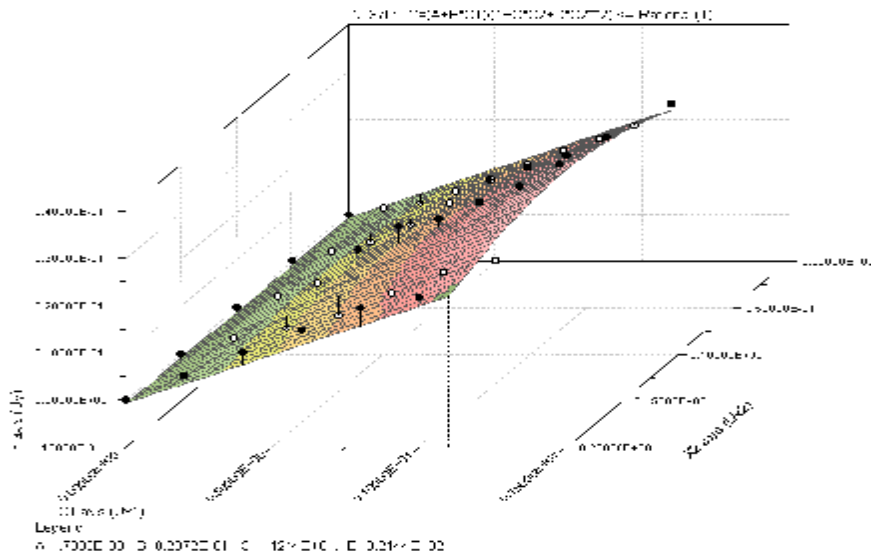**Figure (16) Normalized Pressure –Settlement Surface for Gypseous Soil at Soaked State (Center).**

Figure (17) Normalized Pressure –Settlement Surface for Gypseous Soil at Soaked State (Edge).

Figure (18) Normalized Pressure –Settlement Surface for Gypseous Soil at Dry State (Center).

Figure (19) Normalized Pressure –Settlement Surface for Gypseous Soil at Dry State (Edge).

Eng. & Tech. Journa , Vol.31.Part(A) , No.20,2013   **Prediction of Square Footing Settlement under**
Eccentric Loading on Gypseous Soil through
Proposed Surface for Dry and Soaked States

Figure (20) Normalized Pressure –Settlement Surface for
Gypseous Soil at Soaked State (Center).

Figure (21) Normalized Pressure –Settlement Surface for
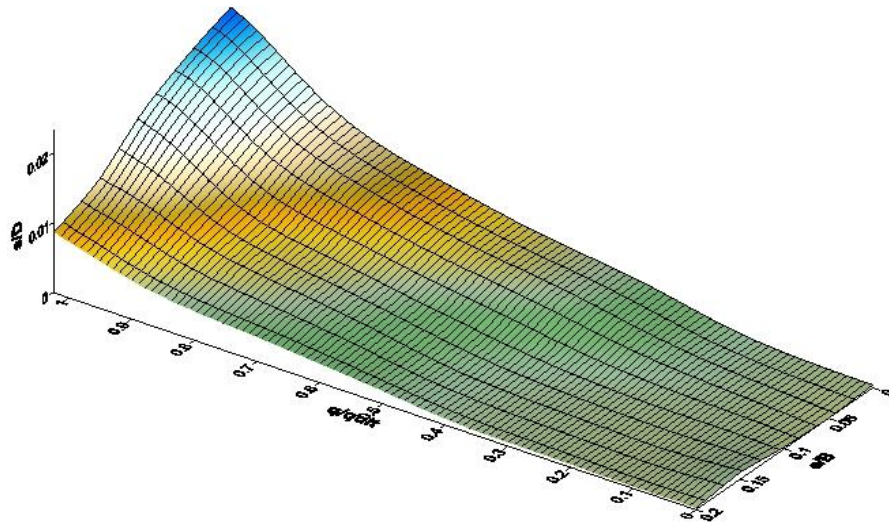**Gypseous Soil at Soaked State (Edge).**

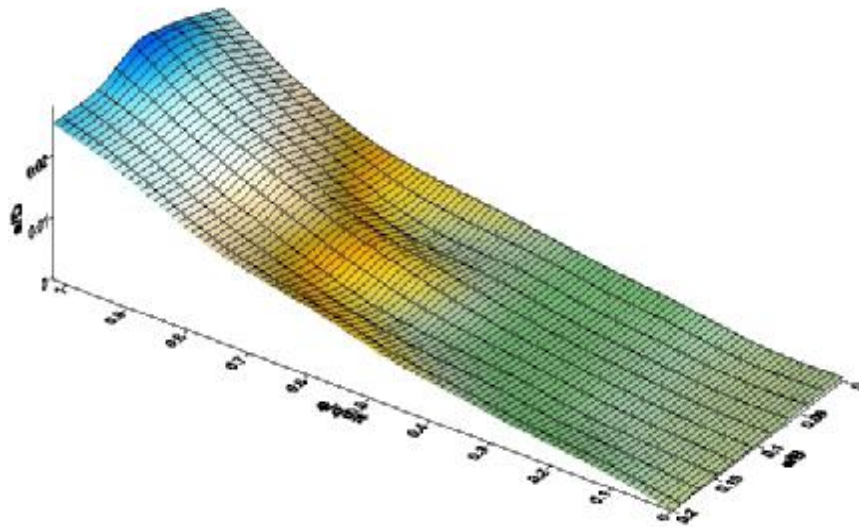**Figure (22) Normalized Pressure –Settlement Surface for Gypseous Soil at Dry State (Center) from ANN.**

Figure (23) Normalized Pressure –Settlement Surface for Gypseous Soil at Dry State (Edge) from ANN.
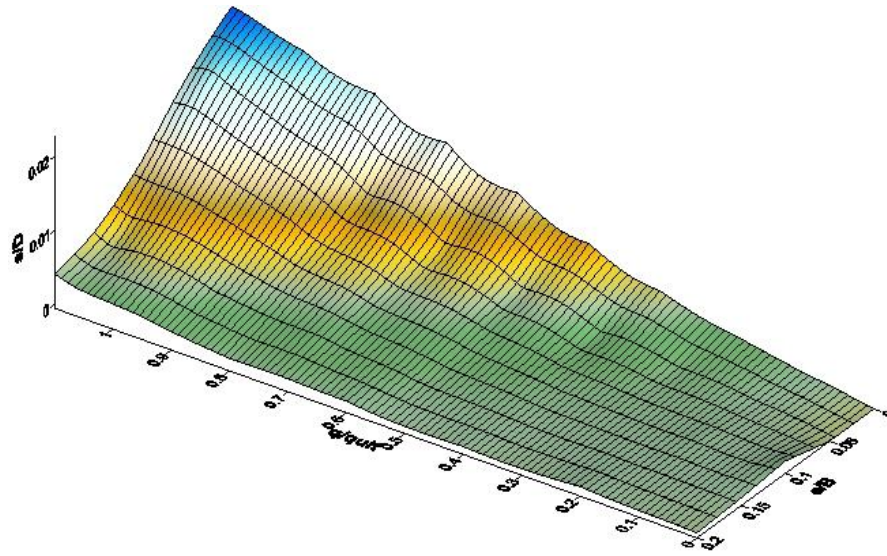
Eng. & Tech. Journa , Vol.31.Part(A) , No.20,2013   **Prediction of Square Footing Settlement under
Eccentric Loading on Gypseous Soil through
Proposed Surface for Dry and Soaked States**

**Figure (24) Normalized Pressure –Settlement Surface for
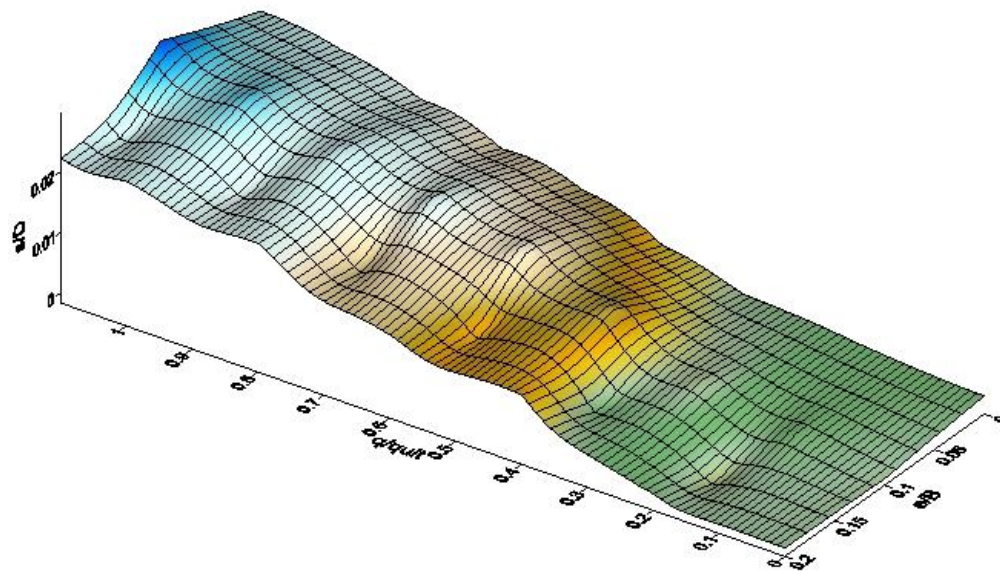Gypseous Soil at Soaked State (Center) from ANN.**

**Figure (25) Normalized Pressure –Settlement Surface for
Gypseous Soil at Soaked State (Edge) from ANN.**